energies

MDPI

Article

Optimizing Load Frequency Control in Standalone Marine Microgrids Using Meta-Heuristic Techniques

Sanath Alahakoon [1], Rajib Baran Roy [1,*] and Shantha Jayasinghe Arachchillage [2,3]

[1] School of Engineering and Technology, Central Queensland University, Rockhampton 4701, Australia; s.alahakoon@cqu.edu.au
[2] Australian Energy Market Operator, Melbourne 3000, Australia; shantha.jayasinghe@utas.edu.au
[3] Australian Maritime College, University of Tasmania, Launceston 7250, Australia
* Correspondence: r.roy@cqu.edu.au

Abstract: Integrating renewable resources into the electrical systems of marine vessels achieves the dual goal of diversifying energy resources and reducing greenhouse gas emissions. The presence of intermittent renewable sources and sudden nonlinear load changes can cause frequency deviations in isolated hybrid marine microgrids. To address this issue, the paper proposes a conventional PID (proportional–integral–derivative)-controller-based LFC (load frequency controller) which is optimized by meta-heuristic optimization algorithms, namely, PSO (particle swarm optimization), GWO (grey wolf optimization) and hybrid PSO-GWO. The proposed LFC was designed using transfer functions of various microgrid components, with ITAE (integral time absolute error) and ITSE (integral time square error) serving as performance indices. The proposed LFC's validation was performed through HIL (hardware-in-loop) real-time simulation using a DS 1104 R&D controller board, with simulation results showing the better performance of the optimized frequency response compared to the nonoptimized LFC controller in terms of rise time, fall time, slew rate and overshoot. The hybrid PSO-GWO algorithm performs better than the other optimization algorithms. The simulation results demonstrate the stability and robustness of the proposed controller. In summary, the proposed PID-controller-based LFC can regulate frequency deviation in standalone hybrid marine microgrids effectively.

Keywords: marine microgrid; load frequency controller; PID; hybrid PSO-BFO algorithm; ITAE; ITSE; HIL

check for updates

Citation: Alahakoon, S.; Roy, R.B.; Arachchillage, S.J. Optimizing Load Frequency Control in Standalone Marine Microgrids Using Meta-Heuristic Techniques. *Energies* **2023**, *16*, 4846. https://doi.org/10.3390/en16134846

Academic Editor: Theofilos A. Papadopoulos

Received: 24 May 2023
Revised: 12 June 2023
Accepted: 18 June 2023
Published: 21 June 2023

Copyright: © 2023 by the authors. Licensee MDPI, Basel, Switzerland. This article is an open access article distributed under the terms and conditions of the Creative Commons Attribution (CC BY) license (https://creativecommons.org/licenses/by/4.0/).

1. Introduction

The greenhouse gas emissions of conventional diesel-generator-powered marine vessels can be significantly curtailed by the integration of renewable resources into marine vessels' electrical systems. The hybridization of renewables with conventional diesel generators can be a feasible option for large marine vessels. Renewable energy with a storage-driven electric system may be applicable for small marine vessels, such as ferries and others. According to the type of marine vessel, there are three types of propulsion systems, namely, the diesel mechanical type, the diesel electric type and the all-electric type. Electric propulsion has the highest efficiency of 68% as compared to 32% and 28% efficiencies for diesel mechanical and diesel electric propulsions [1]. The advancement of battery technology has enhanced the option of using storage along with other power sources in a marine vessel for supporting the dynamic load, especially during cruising. The propulsion load changes drastically with the variation in seawater during bad weather, which necessitates the use of a hybrid power system (a diesel generator with renewables and storage) in a large marine vessel. The concept of the microgrid was initiated by CERTS (the Consortium for Electrical Reliability Technology Solutions) in 1998 [2] to secure reliability and flexibility, attain environmental issues and decentralization, and diversify energy sources by utilizing renewable resources for conventional power systems [3]. The

network-connected mode, the island or isolated mode, and the hybrid mode are three modes of operation for a microgrid [4]. The electrical power system of a marine vessel with various energy-source options, such solar PV (photovoltaics), WTs (wind turbines) [5], fuel cells, ESSs (energy storage systems) and others, can be termed a marine microgrid [6,7]. The marine vessel microgrid is mainly an island or isolated microgrid which can interact with the shoreside electricity grid when the vessel is at berth.

The characteristics of the nonlinear marine load are different from those of other nonlinear loads, such as EVs (electric vehicles) and heavy-duty mining vehicles. The nonlinear propulsion load comprises several rotating types of machinery which consume significant electrical power during the cruising of a marine vessel. The integration of power electronics devices in marine transport systems has enhanced their nonlinear load patterns. The high penetration of intermittent renewables in island marine microgrids increases the complexity and instability. A rapid and abrupt change in nonlinear load causes frequency deviation in a marine microgrid. Since the frequency deviation is related to the real power, the system power [8] is also affected by it. The energy reserve which is provided by storage elements is important in a microgrid due to the low inertia and slow response time of various energy resources. For a marine microgrid, a backup diesel generator and storage element can only support the frequency deviation due to abrupt changes in load, which may not be adequate. Uncertainty, low inertia, complex dynamics, nonlinear structure and [2] intermittency are the prime challenges for a marine microgrid, which may lead to blackout due to frequency deviation [2]. The constantly changing load and generation sources make the electrical power system more complex in marine vessel microgrids. Moreover, marine vessels operate in harsh environments, such as in rough seas or extreme weather conditions, when power fluctuations can be even more severe.

For the efficient operation of [9] marine vessels, the LFC [9] is an important aspect of various power sources based on the isolated marine microgrid. The LFC is imperative for isolated marine microgrids because it is incapable of balancing load from the external power system like a conventional microgrid. The power requirement of a marine vessel constantly changes due to randomly fluctuating dynamic marine load and the integration of intermittent renewable sources. The marine vessel microgrid is often subjected to highly variable load demand due to marine weather and the number of people on board. Since the frequency varies with load, without proper LFC, the load fluctuations can cause the frequency and voltage of the marine microgrid to become unstable, leading to potential equipment damage, power outages and even safety risks. To address these challenges, the LFC in an isolated marine microgrid needs to be highly adaptable and responsive, which requires sophisticated control systems that can quickly detect changes in frequency and adjust the output power accordingly with the load demand. Moreover, the LFC must be able to operate in highly variable marine weather conditions, including rough seas and high winds, and given other environmental factors. Since the utilization of renewable-energy-based hybrid microgrids is increasing to mitigate environmental impacts, it is imperative to implement appropriate LFC to meet the complex and dynamic requirements of marine power systems. The LFC maintains a balance between the generation and load, which ensures stability and reliability in the marine microgrid.

So far, several research works have been conducted on load frequency control on microgrids, and the key findings and limitations of some research works are mentioned in this section. Khooban et al. proposed a modified black-hole optimization algorithm based on [10] fuzzy PD+I LFC which utilizes the linear matrix inequality technique and Lyapunov stability theory [7,11]. The HIL-simulation-based validation demanded better frequency regulation with a reduction in frequency deviation [7]. The performance of the proposed LFC was analyzed for stepwise load [12] variation, which may not be applicable for abrupt load change for a marine vessel in extreme weather [7]. Model predictive control or adaptive control, rather than proportional control, can provide better performance and robustness in real-world applications. The lack of thorough analysis and discussion of the obtained results does not signify the performance of the proposed LFC. Srinivasarathnam et al.

investigated a GWO-algorithm-based [13] LFC for an MMG (multi-microgrid) system using RES (renewable energy sources) and an ESS (energy storage system) [14,15]. According to this paper, the GWO algorithm can significantly improve the LFC performance of the MMG while considering the intermittency of RES and marine load [14,15]. This paper lacks a detailed analysis and interpretation of the proposed LFC. There is no comparative analysis of using GWO with other optimization algorithms. A sensitivity analysis concerning the variation in system parameters is important for assessing the robustness of the proposed [16] approach. An LFC for a wind–diesel hybrid microgrid system with [17] battery and super-capacitor energy storage has been proposed by Mi et al. [18]. The objective of the proposed LFC was to reduce [19] frequency deviation and restore stability during system disturbances, and the system was validated by an RTDS (a real-time digital simulator) in multiple scenarios [18]. The paper does not provide an in-depth analysis of the [20] performance and limitations of this technology in a wind–diesel hybrid power system [21]. Therefore, more research is needed to validate the proposed strategy by considering a real-world scenario.

Coban et al. discussed the potential benefits of using a combination of battery and pumped hydro energy storage for load frequency control in microgrid systems [22]. The simulation results revealed that the proposed strategy maintains the frequency of the microgrid system [23] within acceptable limits at various loads [22]. The proposed PID-based control strategy does not analyze the stability of the microgrid system under different operating conditions and [16] compare its performance with other advanced control topologies. Modal et al. proposed a direct search-and-butterfly-optimization-algorithm-driven FOPID (fractional-order proportional–integral–derivative) frequency controller [24] for a hybrid shipboard microgrid system [25]. The proposed controller uses the non-integer order method and the least common multiple method to convert the closed loop nonidentical fractional-order frequency control system [25]. A relative comparison of various control strategies and optimization algorithms was also provided for the shipboard microgrid system to represent the suitability of the proposed approach [25]. No experimental validation was provided for the proposed simulation-based frequency control approach to evaluate its effectiveness in a practical shipboard microgrid system. Further research is required to determine the performance of the proposed frequency control method [26]. Kwon et al. proposed an LFC-based power management strategy to maintain a balance between power generation and consumption for shipboard DC hybrid power systems [27] by using the low pass for each power source [27]. The simulation-based approach implies an effective load distribution scheme in terms of charging/discharging the intervention of hybrid systems [27]. The paper lacks a relative comparison of the proposed LFC-based power management strategy with other existing power management strategies.

A rigorous test-driven load frequency control [28] approach for a hybrid maritime microgrid system is presented by Latif et al. which considers the nonavailability of renewable resources, concurrent random [29] wind power and load demand [30]. The comparative performance analyses of advanced PID-based controllers, where operational parameters are optimized by various meta-heuristic optimization algorithms, are discussed [30]. The grasshopper-algorithm-tuned PI-(1 + PD) controller performs better [30] when the sensitivity assessment is performed under variations in wind generation, droop factor, the inertia constant and loading without re-optimizing the optimal base-condition values [29,30]. The simulation validation is not sufficient to justify the performance of the proposed controller [31] in real field applications. The linear matrix inequality technique and the Lyapunov-stability-theory-based [32] LFC were proposed based on the hybrid maritime microgrid of Vafamand et al., which considers the effects of the sensor-to-controller and controller-to-actuator delay [32,33]. The simulation-based comparative validation justifies the effectiveness of the proposed approach, which outperforms other methods in terms of frequency regulation and stability [33]. The paper does not consider the impact of external factors, such as an abrupt change in propulsion load during bad weather and the

intermittency of renewable energy sources, on the performance of the proposed centralized control method [34].

The literature reviewed does not take into account the fluctuating and sudden load variations experienced in marine vessels during turbulent sea conditions when discussing the proposed LFC systems for microgrids. The performance of the proposed controllers has not been discussed using conventional performance indices to justify the applicability of the controllers for mitigating frequency deviation. These research papers do not validate the robustness of the controller due to unpredictable marine load fluctuations and intermittent renewable sources, which issue is addressed with the proposed LFC. The isolated marine microgrid is highly responsive to unstable frequencies due to abrupt changes in load during harsh marine weather. Thus, it is necessary to have a highly adaptable and responsive LFC in an isolated marine microgrid that can detect changes in frequency and adjust the output power based on the demand of the load. For frequency stability, it is imperative to implement suitable LFC for the complex and dynamic loads of marine vessels. In this paper, a robust PID-controller-based LFC is proposed for an isolated hybrid marine microgrid whose parameters are optimized by meta-heuristic optimization algorithms. The proposed LFC considers the intermittency of renewable resources and abrupt change in marine vessel load to manage frequency fluctuations. Performance indices, such as ITSE and ITAE, are used for the validation of the proposed LFC.

2. Conventional LFC Topology

The load frequency control technique is effectively used for frequency regulation in the power system [35]. The selection of the controller and its parameters greatly affects the performance of the LFC. The LFC restores the mismatch between the generation and load for the specified control area of the power system [36] and minimizes the transient deviations with zero steady-state error. The main purpose of the LFC controller is to make fine adjustments in system frequency to the reference frequency. The rigorous and repeated process of attaining zero frequency deviation ensures a balance between the generation and load [37]. A controller is a device that is equipped with general proportion, integration and derivation gains [38], which can be defined by various controller design approaches [39]. Several control topologies are used for designing LFC systems according to system requirements. The commonly used control topologies are discussed in this section, which assisted in designing the proposed LFC for marine microgrids.

2.1. Classical Control

The classical control approach is a traditional method of designing control systems that uses analytical methods to design feedback control systems to regulate the behavior of physical systems predictably. In this method, the controller is designed to provide a closed-loop system [40] that responds to inputs and outputs, and the system's response is analyzed in terms of stability, accuracy and speed of response. The classical control approach is Laplace-transformation-based, representing the system's behavior in terms of a transfer function to attain the desired system performance. In classical control, the PI (proportional–integral) and PID controllers are widely used, where the integral square error technique [38] is used for LFC, which can be an effective solution for maintaining stable frequency and power balance for marine microgrids [38]. The controller should be able to adjust the power output of the [8] different sources in response to changes in the load demand [41] while maintaining the frequency and power balance within the microgrid. Though this control approach is widely used in various engineering applications, it has some limitations, such as difficulty in handling nonlinear systems and distributive rejection. Modern control approaches, such as state-space control and adaptive control, have been developed to overcome these limitations and provide better control performance.

2.2. Adaptive Control

The adaptive control technique is useful in controlling complex systems where traditional control methods may not be effective. This technique involves the design and analysis of controllers that adapt to the changing behavior of controlled systems for various engineering applications. This technique involves designing a controller that can adapt to the changing behavior of the controller system and maintain stability and performance. The adaptive controller is more complex than the traditional PID controller [42] which can monitor process parameters and predict and detect failures. An adaptive-control-based LFC system can be an effective solution for maintaining stable frequency and power balance within a marine microgrid while also adapting to changes in the system dynamics and handling uncertainties caused by the changing ocean conditions. The adaptive controller should be designed and tested to estimate the uncertain parameters of the system and update the control action accordingly, ensuring the reliability and stability of the microgrid operation. The merits of this technique are adaptability, robustness and improved performance, whereas its demerits are its complexity, the computational burden and tuning difficulty. The suitability of adaptive control for a particular application [43] depends on the specific system's requirements and characteristics.

2.3. Model Predictive Control

MPC (model predictive control) is an advanced control strategy that has gained in popularity in various industrial processes [44] over the years. MPC is a feedback control that uses a dynamic mathematical model to predict system behavior over a certain horizon and then calculate the control actions that optimize a certain objective function over this prediction horizon. It can attain a wide range of control objectives, including set-point tracking, disturbance rejection and the optimization of energy consumption or product quality. MPC can also improve the efficiency and productivity of the controlled process, resulting in reduced energy consumption and lower operating costs. MPC is an emerging trend for LFC in power systems, where frequency mismatch is predicted in advance before its effect on the system [45,46]. An MPC-based LFC system can be an effective solution for maintaining stable frequency and power balance within a marine microgrid, while also optimizing the utilization of the available power sources. The MPC controller should be designed and tested to handle constraints on the power sources and loads while also optimizing the performance of the system [47]. This can lead to the improved efficiency, reliability and sustainability of the marine microgrid operation. The drawbacks of MPC are computational complexity, model errors, tuning complexity, computational time constraints, offline computation, high implementation costs and limited robustness. For better performance, artificial-intelligence-based neural networks and fuzzy logic are now used in MPC for optimal tuning of the controller's parameters [48].

2.4. Robust Control

Robust control provides stable and predictable performance in the presence of uncertainties and disturbances, such as modeling errors, parameter variations and [49] environmental disturbances. The goal of robust control is to ensure that the controlled system behaves consistently under different operating conditions, such as changes in the environment or variations in the system parameters. This control technique is now widely used in many fields of engineering, including aerospace, automotive and process control. Several techniques are used in robust control, such as robust stabilization, robust performance and H-infinity control. The key challenge in robust control is the tradeoff between performance and robustness, which needs to be considered in designing a robust controller [38]. The robust controller for the LFC of a microgrid should be able to handle uncertainties and disturbances caused by changing ocean conditions to ensure the reliability and stability of the microgrid's operation. A common robust control technique used for LFC is H∞ control, which minimizes the worst-case performance of the system under uncertain conditions. In robust control, the uncertainties in the system are considered to be bounded and known,

but for real-world systems, uncertainties are difficult to model and are time-varying. Therefore, this control technique may not be suitable for systems that are highly nonlinear with complex dynamics. In such cases, more advanced control techniques, such as adaptive or intelligent control, may be necessary to achieve optimal performance. For better set-point tracking ability, regulation, accuracy and robustness, a hybrid FFOPI-FOPD (fuzzy fractional order proportional integral—fractional order proportional derivative) controller [35], a 2DOF-IDD (two degrees of freedom with integral and double derivative function) robust controller and a 3DOF (three degrees of freedom) PID robust controller [38] have been proposed by different researchers [50,51].

2.5. Internal Mode Control

The feedback control technique based on internal mode control (IMC) relies on the principle that a good control system must be able to reject disturbances and track set points. The mathematical model used in IMC consists of a process transfer function and a model of the controller. The controller model is used to estimate the future controller output based on the current process input and the past controller output. The process transfer function is used to predict the process response to changes in the controller output. The controller adjusts the control signal to maintain the desired process variable at its set point by comparing the predicted process response with the actual process response. The IMC strategy has several advantages: first, it provides a simple and intuitive method for designing a feedback controller; second, it is robust to model uncertainties and process disturbances; and third, it provides good set-point tracking and disturbance rejection performance. The IMC-based LFC controller can be designed based on the internal model of the microgrid. The controller needs to be capable of handling load disturbances and uncertainties with changes in the power sources and loads. The IMC-based LFC system may be an effective solution for maintaining stable frequency and power balance within a marine microgrid while also ensuring optimal utilization of the available power sources. The limitations of this technique are its model-dependency, difficult tuning, unsuitability for nonlinear processes, difficulties in dealing with time delays and computational complexity. The intelligent soft-computing-based meta-heuristic optimization approach is a new trend for internal mode control for obtaining fast and stable responses for PID controllers. The system dynamics of internal mode control are represented in the form of a sliding-surface design by the optimal sliding-manifold technique via state-variable transformation to obtain fast response and robustness with respect to system parameter uncertainties [38,52].

2.6. Meta-Heuristic Optimization Control

Meta-heuristic optimization algorithms are a class of optimization techniques that leverage the principles of natural and social systems to solve complex problems. These algorithms employ stochastic search procedures that explore the search space of a problem to find the optimal solution. The search procedure typically involves a set of rules that govern the movement of the search agents or particles. Since meta-heuristic optimization algorithms offer a robust and efficient approach for solving complex control systems, the application of this in engineering and other fields is increasing. Meta-heuristic-optimization-based LFC is designed to optimize the control parameters of a microgrid in real time to achieve optimal performance and ensure system stability [53,54]. One of the key benefits of meta-heuristic-optimization-based LFC is its ability to quickly adapt to changing system conditions, which is essential for maintaining stability in a dynamic microgrid. Additionally, these systems can provide near-optimal or optimal solutions to complex optimization problems that are difficult to solve using traditional methods. Generally, the performance of the hybrid meta-heuristic algorithm is better than [54] that of a single meta-heuristic algorithm. For reliable and robust controller design, the optimization algorithm helps in attaining better response with a low overshoot and setting time [55]. The research in this area will initiate further advancement in the application of meta-heuristic optimization algorithms for LFC and other power-system stability applications.

3. Marine Microgrid System Representation

This paper proposes an LFC for a hybrid marine microgrid consisting of multiple sources, such as fuel cells, solar PV, diesel generators, and BESSs (battery energy storage systems). The primary sources of electricity to fulfill the load demand are a fuel cell and solar PV, while the diesel generator serves as a backup electricity source to meet the peak demand. The BESS is used to regulate the system frequency by charging and discharging electricity as per the system's requirements. The electricity sources and loads of the standalone marine microgrid are represented by their respective transfer functions for analyzing frequency deviations with changing loads.

3.1. Diesel Generator Model

The basic transfer-function-based diesel engine governor model is shown in Figure 1 [56], where the actual speed, ω_r, is compared with the reference speed, ω_{ref}. The prime-mover mechanical torque is derived as a percentage of the nominal power and provided by the output of the actuator [57]. The mechanical torque is [57] transferred to the engine delay block of time delay, Ta. The mechanical power, P_{mec}, is the product of the time delay and the rotor actual angular speed, ω_r, which is the input for the mechanical part of the synchronous generator. The error signal is applied to the input by using a feedback path which represents the model as a second-order system.

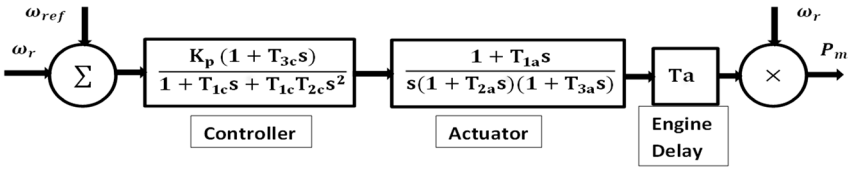


Figure 1. Diesel engine governor model.

The transfer function for the controller is represented by Equation (1).

$$H_c(s) = \frac{K_p\ (1 + T_{3c}s)}{1 + T_{1c}s + T_{1c}T_{2c}s^2} \tag{1}$$

where K_p denotes gain and T_{1c}, T_{2c} and T_{3c} represent controller time constants [57].

The actuator transfer function can be defined by Equation (2) [57].

$$H_a = \frac{1 + T_{1a}s}{s(1 + T_{2a}s)(1 + T_{3a}s)} \tag{2}$$

where T_{1a}, T_{2a} and T_{3a} represent actuator time constants.

3.2. Solar PV Model

The transfer function of a solar cell describes the relationship between the input and output signals of the cell [58]. In the case of a solar cell, the input signal is the incident light intensity, and the output signal is the generated electrical current or voltage. The transfer function of a solar cell is generally nonlinear and can be affected by various factors, such as temperature, shading and the spectral distribution of the incident light. The most commonly used mathematical model for the transfer function of a solar cell is the Shockley–Queisser model, which provides a theoretical upper limit for the efficiency of a solar cell [58]. The Shockley–Queisser model expresses the I-V (current–voltage) relationship of a solar cell, which is represented by Equation (3).

$$I = I_L - I_o\left[e^{(q(V+IR_s)/nK_BT)} - 1\right] - (V + IR_s)/R_{sh} \tag{3}$$

where I is the output current, I_L is the light-generated current, I_o is the diode saturation current, q is the elementary charge, V is the output voltage, R_s is the series resistance, R_{sh} is

the shunt resistance, K_B is the Boltzmann constant, T is the temperature and n is the ideality factor.

The transfer-function-based solar PV model is depicted in Figure 2 [14], where the input (solar irradiance) and output (dc voltage) are represented by $\Delta\varphi$ and ΔP_{PV}, respectively. The first-order transfer function for the solar cell, inverter and filter are represented by Equations (4)–(6), respectively.

$$H_{PV} = \frac{K_{PV}}{1 + sT_{PV}} \tag{4}$$

$$H_I = \frac{E}{1 + T_I s} \tag{5}$$

$$H_{FL} = \frac{1}{1 + T_{FL} s} \tag{6}$$

where T_{PV}, T_I and T_{FL} are the time constants for the solar PV, inverter and filter, respectively. The solar PV and inverter constants are represented by K_{PV} and E, respectively. The standard solar irradiation is considered as 1000 W/m^2.

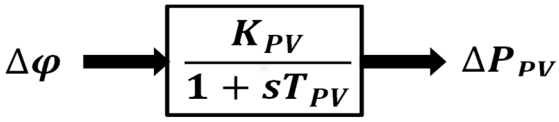


Figure 2. Solar PV model.

3.3. Fuel Cell Model

The dynamic model of a fuel cell is a mathematical representation that describes the behavior of the fuel cell over time [59], including the changes in voltage, current and other variables. There are different approaches to modeling a fuel cell, and the equations may vary depending on the assumptions and simplifications made. The simplified dynamic model of a fuel cell is based on the electrochemical reactions that occur within it [60]. The steady state V-I characteristics of a PEM (proton-exchange-membrane) fuel cell can be represented by Equation (7).

$$V_{cell} = E_N - V_a - V_C - V_{ohm} = V_{St} - V_{tr} \tag{7}$$

where V_{cell}, E_N, V_a, V_c, V_{ohm}, V_{st} and V_{tr} denote the output of the fuel cell, the reversible voltage of the fuel cell (also termed the thermodynamic potential), the voltage drop due to the activation of the anode and cathode (also termed the activation overvoltage), the voltage drop resulting from the reduction in the concentration of the reactant gases or from the transport of mass of oxygen and hydrogen (also termed the concentration overvoltage), the ohmic voltage drop resulting from the resistance of the conduction of protons through the solid electrolyte and of the electrons through its path (also termed the ohmic overvoltage), the steady-state component of the cell voltage and the transient component of the cell voltage [61].

The transfer function of a fuel cell is a mathematical representation that relates the input to the output of the fuel cell. The transfer function is typically expressed in a Laplace domain, and it can be derived from the dynamic model of the fuel cell. The transfer-function-based fuel cell model is demonstrated by Figure 3 [62]. The general transfer function of a fuel cell system is represented by Equation (8).

$$G(s) = V(s)/I(s) \tag{8}$$

where G(s) is the transfer function, V(s) is the Laplace transform of the voltage and I(s) is the Laplace transform of the current. The transfer function provides a useful tool for analyzing the performance of the fuel cell under different operating conditions.

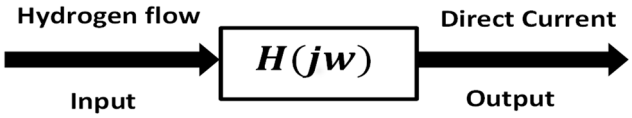


Figure 3. Fuel cell model.

The first-order transfer function of a fuel cell [63] with an inverter and filter can be represented by Equations (9)–(11).

$$H_f = \frac{1}{1 + T_f s} \tag{9}$$

$$H_i = \frac{A}{1 + T_i s} \tag{10}$$

$$H_{fl} = \frac{1}{1 + T_{fl} s} \tag{11}$$

where T_f, T_i and T_{fl} are the time constants of the fuel cell, inverter and filter, respectively. A represents the inverter constant. The standard H_2 intake of the fuel cell is considered as 50 kg.

3.4. BESS Model

The rotating masses of conventional frequency-regulating devices of diesel engine generators have high inertia, which is not appropriate for a system with abrupt and dynamic load variation, such as a marine vessel. A BESS can provide dynamic and fast frequency-regulating support by remaining in charging and discharging modes. The first-order transfer function model of the BESS is represented in Figure 4 [2]. K_{BESS}, T_{BESS}, Δf and ΔP_{BESS} represent the operational constant, time constant, input (chemical energy) and output (electrical energy), respectively. The BESS is in charging and discharging modes when the change in frequency is positive and negative, respectively.



Figure 4. BESS model.

4. Proposed LFC Design Methodology

Due to the nonlinearity and abrupt changes in load demand, selecting an appropriate controller to restore the system frequency of the marine microgrid is crucial. Designing an LFC with sensitivity and robustness is essential for maintaining a balance between electricity generation and load demand [34]. Compared to conventional microgrids, the multiple electricity generation sources in marine microgrids make the LFC more complex, highlighting the need for further research. While numerous studies have been conducted on LFC for microgrids, only a few have focused on the standalone marine microgrid. Most previous research has proposed meta-heuristic optimization approaches for LFC which lack the linearization needed to define optimal controller parameters [64]. Furthermore, the proposed controllers' limitations include high overshoots and setting times and low convergence, indicating the need for further research in this area.

This paper proposes a multivariable optimal robust control approach for LFC in an isolated marine microgrid [65]. The optimal control design minimizes a performance index related to the dynamic system's variables. The primary objective of the optimal control design is to determine the optimal control law, u*(x, t), which transfers the system from its initial state to the final state while minimizing the given performance index. The control design selects the best performance index that balances performance and control costs. The quadratic performance index is the most commonly used optimal control design,

which depends on the minimum error and minimum energy criteria [66]. Initially, the paper analyzes the process of optimal control design for a simple LQR (linear quadratic regulator) with a quadratic performance index for a single-source linear system represented by Equation (12). The feedback gain vector is determined using Equation (13). Equation (14) defines the minimization value of the quadratic performance index, J.

$$\dot{x}\,(t) = Ax(t) + Bu(t) \tag{12}$$

$$u(t) = -K(t)x(t) \tag{13}$$

$$J = \int_{t_0}^{t_f} (x'Qx + u'\,Ru)dt \tag{14}$$

In this context, Q and R are positive semi-definite and real symmetric matrices, respectively, with non-negative principal minors. The selection of Q and R determines the relative weighting of individual state variables and control inputs. The Lagrange multipliers method is typically utilized for a formal solution. Solving the constraint problem of Equations (12)–(14) requires an n vector of Lagrange multipliers, λ. The minimization of the unconstrained function is expressed by Equation (15).

$$\mathcal{L}(x,\ \lambda, u, t) = \left[x'Qx + u'\,Ru\right] + \lambda'\left[Ax + Bu - \dot{x}\right] \tag{15}$$

The optimal values, which are indicated by the superscript *, are obtained by equating the partial derivatives to zero. The values of $\dot{x}^*$, u^* and $\dot{\lambda}$ can be obtained from Equations (16), (17) and (18), respectively.

$$\frac{d\mathcal{L}}{d\lambda} = AX^* + Bu^* - \dot{x}^* = 0 \qquad \text{So, } \dot{x}^* = AX^* + Bu^* \tag{16}$$

$$\frac{d\mathcal{L}}{du} = 2Ru^* + \lambda'\,B = 0 \qquad \text{So, } u^* = -\frac{1}{2}\,R^{-1}\lambda'B \tag{17}$$

$$\frac{d\mathcal{L}}{dx} = 2x'^*Q + \dot{\lambda}' + \lambda'B = 0 \qquad \text{So, } \dot{\lambda} = -2Qx^* - A'\lambda \tag{18}$$

By considering a symmetric, time-varying positive definite matrix p (t), λ can be defined by Equation (19).

$$\lambda = 2p(t)x^* \tag{19}$$

By substituting Equation (13) into Equation (19), the optimal closed-loop control law is represented by Equation (20).

$$u^*(t) = -R^{-1}B'p(t)x^* \tag{20}$$

The derivate of Equation (19) can be defined by Equation (21) and finally equating Equation (19) with Equation (21), and Equation (22) can be obtained.

$$\dot{\lambda} = 2(\dot{p}x^* + p\dot{x}^*) \tag{21}$$

$$\dot{p}(t) = -p(t)A - A'p(t) - Q + p(t)BR^{-1}B'p(t) \tag{22}$$

The matrix Riccati equation is presented as Equation (22) and is associated with the value of 21. As the boundary condition states that p(tf) equals zero, Equation (22) needs to be integrated in reverse chronological order. When employing a numerical solution that operates forward in time, it is possible to substitute a dummy time variable, $\tau = t_f - t$, for t [67]. Upon solving Equation (22), the solution to the state Equation (16) is connected to

the optimal control Equation (20) [67]. The optimal controller gain represents state variable feedback that varies with time and can be challenging to solve without the aid of specialized software, such as MATLAB [67]. To manually approach the solution, an alternative method involves substituting the time-varying optimal gain, K(t), with its constant steady-state value [68]. For linear time-invariant systems where the process extends infinitely with $\dot{p} = 0$ and $t_f = \infty$, the Riccati equation (Equation (22)) can be expressed as Equation (23) [68].

$$pA + A'p + Q - pBR^{-1}B'p = 0 \quad (23)$$

The design of robust LFC differs significantly from conventional control design methods that directly select the gain matrix, K. Instead, design parameters, such as weight matrices, Q and R, are chosen first, and then the feedback gain, K, is determined using matrix design equations. Typically, computer simulations are utilized to obtain closed-loop time responses. If unsatisfactory responses are obtained, the design and simulation process is repeated by assigning new values of Q and R. To achieve closed-loop stability for a multi-loop control system, such as an LFC system, the LQR (linear quadratic regulator) enables all control loops to be closed simultaneously. Figure 5 illustrates the schematic diagram of the transfer-function-based optimal LFC design for the isolated marine microgrid, ensuring both robustness and stability.

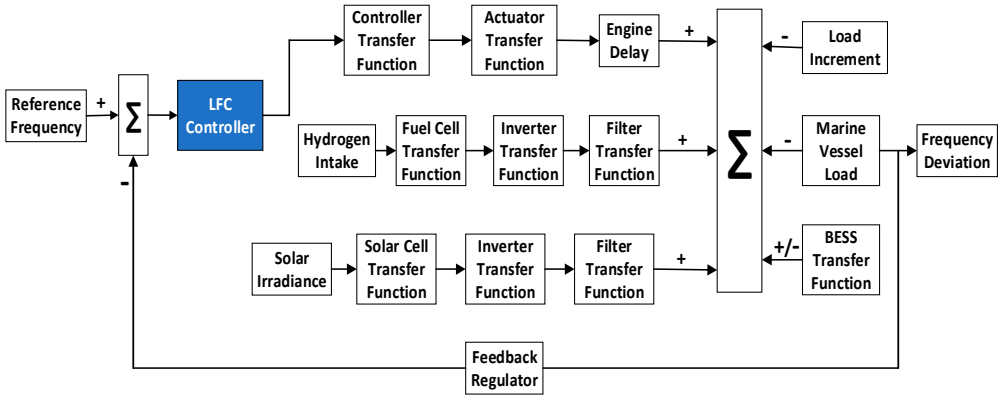


Figure 5. Schematic diagram of proposed LFC.

5. Justification of Using Meta-Heuristic Optimization Algorithm

The mathematical optimization problem can be categorized into two main types: convex optimization problems and nonconvex optimization problems [69]. In a convex optimization problem, any local optimum is a global optimum which ensures the convergence to the solution of the problem [69]. In the case of a nonconvex problem, achieving convergence to the solution is hindered because a local optimum does not necessarily correspond to the global optimum; as a result, solving this type of problem often necessitates the use of heuristics [70]. The derivative-based optimization algorithm, also known as the gradient-based optimization algorithm, is a class of optimization methods that utilize the derivatives of a function to find the minimum or maximum of that function [71]. This algorithm is commonly used in machine learning, numerical optimization and various other fields. The basic idea behind this algorithm is to iteratively update the parameters or variables of a function based on the direction indicated by the derivative [72]. The derivative provides information about the slope or rate of change of the function at a particular point, which allows the algorithm to make adjustments that move closer to the optimal solution [72]. The gradient descent method, Newton's method, the conjugate gradient method and the quasi-Newton method are commonly used derivative-based optimization algorithms [71,72]. These algorithms demonstrate efficient handling of high-dimensional problems and exhibit notable effectiveness when optimizing smooth and differentiable functions [72]. However, challenges may be encountered in nonconvex optimization problems with multiple local optima or when the function has discontinuities or other irregularities [71].

The meta-heuristic optimization algorithm is a type of search algorithm which is designed to find optimal or near-optimal solutions for complex optimization problems [73]. This algorithm explores the search space extensively and escapes local optima in order to tackle problems with complex or multimodal landscapes [74]. The algorithm does not require explicit problem knowledge or assumptions about the objective function; rather, it utilizes heuristics or search strategies to guide the search process towards promising regions of the search space [75]. Its operation is based on the concept of a population of candidate solutions or individuals which iteratively evolve and manipulate this population to generate new potential solutions [74,75]. Each iteration typically consists of three key steps; evaluation, exploration and selection [73]. Some popular meta-heuristic optimization algorithms are genetic algorithms (GAs), particle swarm optimization (PSO), grey wolf optimization (GWO), ant colony optimization (ACO), simulated annealing (SA) and differential evolution (DE). Due to their versatility, resilience to noise and capability to handle nondifferentiable or black-box functions, these optimization algorithms find extensive application in various domains such as engineering design, scheduling, resource allocation, data mining, and more [74]. However, they may require more computational resources and may not guarantee global optimality [75].

The derivative-based optimization algorithm excels in efficiency, exploitation of local optima and utilization of problem-specific knowledge, but it is limited by its sensitivity to initial conditions, requirements of differentiability and assumptions of convexity [76], whereas the meta-heuristic optimization algorithm offers global search capabilities, versatility, robustness and parallelizability, though it may be slower in operation, lack problem-specific knowledge and exhibit nondeterministic convergence [76]. The choice between these optimization algorithms depends on the nature of the optimization problem, the available problem information and specific requirements of the application. For the proposed LFC, the meta-heuristic optimization algorithm is more suitable than the derivative-based optimization algorithm in terms of problem-specific information, related assumptions of objective function and robustness. PID controllers are extensively employed in process control applications to regulate system outputs with respect to desired set points [58]. Tuning PID controllers involves adjusting three parameters: the proportional gain, the integral time constant and the derivative time constant, with the goal of optimizing controller performance. The meta-heuristic optimization algorithm can be used to optimize the controller parameters. This paper proposes a robust and reliable LFC system for marine microgrids based on a straightforward PID approach. The PID controller's parameters are optimized using PSO, GWO and hybrid PSO-GWO algorithms to analyze the frequency deviation response.

Grey wolf optimization (GWO) is a meta-heuristic optimization algorithm inspired by the hunting behavior of grey wolves in nature, which is applied to various optimization problems, demonstrating its effectiveness in handling diverse and challenging optimization scenarios [77]. It is designed to find optimal or near-optimal solutions for complex optimization problems. The algorithm mimics the social hierarchy and hunting strategies of a wolf pack to explore and exploit the search space effectively [78]. The GWO employs three main steps, which are encircling prey, searching for prey and attacking prey [77]. It uses the concepts of alpha, beta and delta wolves to represent the best solutions found up to a certain point in time [78]. Its attributes, such as versatility, simplicity, efficiency of exploration and fewer control parameters, make it a versatile optimization algorithm which can be applied to various types of optimization problems, including continuous, discrete and combinatorial problems [77,78]. The demerits of this algorithm are lack of problem-specific knowledge, nondeterministic convergence, computational resource requirements and lack of global optimality, which hiders it in solving problem-specific optimization problems [77,78].

The PSO algorithm is a powerful method for non-smooth global optimization, which is widely applied in complex power-system optimization problems [79]. It employs a bio-inspired approach to find optimal solutions in the search space [80]. Like other derivative-

free optimization algorithms, PSO excels at solving non-smooth global optimization problems [79]. Its simplicity, ease of implementation and limited parameter requirements (one inertia weight factor and two acceleration coefficients) make it more favorable than other meta-heuristic optimization algorithms [80]. Unlike traditional methods, the impact parameters of PSO are less sensitive to the objective function [43]. PSO also demonstrates robust convergence with less dependence on initial parameters, offering high-quality solutions, faster computation and stable convergence characteristics compared to stochastic methods [79,80].

The hybridization of the PSO and GWO algorithms offers several advantages in solving optimization problems. The hybrid PSO-GWO algorithm retains a balance between exploration and exploitation which leads to improved convergence and better-quality solutions [81]. PSO excels in exploring the search space and discovering diverse solutions, while GWO is effective in exploiting the best solutions found up to a given point [54]. PSO may struggle in escaping local optima, while GWO may encounter challenges in fully exploring the search space [54]. The hybrid approach leverages the strengths of both algorithms by mitigating their limitations and enhances the overall optimization performance [81]. The hybrid algorithm can benefit from the complementary search strategies of PSO and GWO. PSO utilizes the concept of social interactions among particles to share information and guide the search, while GWO imitates the leadership hierarchy in wolf packs to guide the search process [54,81]. By combining these strategies, the hybrid algorithm can achieve a more effective and robust search. To utilize enhanced exploration and exploitation capabilities, improved convergence and better optimization results [54,81], the hybrid PSO-GWO algorithm is used for the proposed LFC. The pseudo-code of the hybrid PSO-GWO algorithm is presented in Algorithm 1, which depicts the functional steps for optimizing the controller parameter.

Algorithm 1. Pseudo-code of the hybrid PSO-BFO algorithm

```
Create population randomly
Set a small probability rate, p
Fix maximum iterations and initiate iteration count itr = 0
Run PSO for fitness evaluation of all particle
Sort and index fitness of each particle
If itr = itrmax
stop
      else update particle velocity and position
end if
for current particle
if rand (0, 1) < p, then set the values a, A and C (A and C are coefficient vectors and a is error
introduced to avoid premature convergence for avoiding local minima)
            else run PSO for fitness evaluation of all particle
end if
Evaluate the fitness of all wolves
Update position of α, β, δ wolves X_α, X_β and X_δ
      if itr < itrmax
            Calculate new position of wolves, X(t + 1)
            Substitute this position to PSO particles
            Run PSO
            else update the position of wolf
            end if
end for
Stop if optimal parameters of the PID controller is obtained or repeat the process
```

6. Objective Function, Performance Parameters and Optimization Indices

The objective of the proposed LFC is to optimize the parameters of the PID controller by minimizing the error, which is the difference between the reference input and the controlled variable. The reference input is the reference frequency, whereas the controlled

variable is the frequency deviation. The parameters of the PID controller are optimized by the PSO, GWO and hybrid PSO-GWO algorithms. The hybrid algorithm combines the strengths of both PSO and GWO to enhance the search performance and optimize the parameters of the PID controller. PSO harnesses the power of social interactions among particles to share information and guide the search process, whereas GWO emulates the leadership hierarchy observed in wolf packs to effectively guide the search. The search agent is considered 50, and the search space dimension is 20–40 CH (cluster head). Two performance indices, ITSE and ITAE, minimize the error signal between the reference frequency and the system frequency so that the frequency deviation reduces to zero. The ITAE enhances reference tracking and improves disturbance rejection, while the ITSE reduces the rise time, overshoot and oscillation. Equations (24) and (25) represent the error minimization of two performance indices.

$$\text{Min ITAE} = \text{Min} \int_0^{T_s} t|e(t)|dt \tag{24}$$

$$\text{Min ITSE} = \text{Min} \int_0^{T_s} te(t)^2 dt \tag{25}$$

where t is the time, e(t) is the error signal and Ts is the simulation time.

Four common performance indices, namely, ISE (integral square error), IAE (integral absolute error), ITSE and ITAE, are employed to assess the PID controller's performance [82]. These performance measures, ISE, IAE, ITSE, and ITAE, are also commonly utilized to fine-tune the PID controller's parameters [83]. ISE quantifies the integral of the squared error between the set point and process variable over the entire control interval, while IAE measures the integral of the absolute error over time [84]. ITSE combines ISE and the integral of the squared controller output over time. ITSE represents the integral of the squared error between the set point and process variable, along with the integral of the square of the controller's output throughout the control interval. Similarly, ITAE combines IAE and the integral of the absolute value of the controller's output over time [85]. ISE and ITSE are preferred when minimizing error is the primary concern, whereas IAE and ITAE are suitable for reducing overshoot and oscillation. For the proposed LFC in this paper, ITAE and ITSE serve as the performance indices.

The robustness and reliability of the LFC controller [31] rely on achieving near-zero frequency deviation with load variations in the marine microgrid—a goal accomplished by the proposed controller. The quality of a controller's steady-state response is determined by a low overshoot and settling time. Linearizing the nonlinear transfer-function-based marine microgrid system is necessary to obtain the desired stable response with near-zero frequency deviation. In this study, a MATLAB Simulink-based LFC model of the marine microgrid system was employed to analyze frequency deviation under load variation. The PID parameters were optimized using an objective function and optimization algorithms coded in MATLAB. The MATLAB linearization toolbox facilitated the linearization of the nonlinear microgrid plant model, initially selecting PID parameters, which were later optimized using the optimization algorithm to achieve a controller response with fast convergence and a low settling time. Meta-heuristic optimization techniques were applied to optimize the parameters of the conventional PID controller for the proposed LFC [16]. Real-time validation was conducted in the dSPACE environment, where load variation was introduced from an external source and the frequency deviation was observed using an oscilloscope. The DS 1104 R&D controller board, featuring input/output (I/O) interfaces and a real-time processor on a single board, which was utilized can be connected to a computer. The RTI (real-time interface) manages the MATLAB Simulink diagram and generates the model code via Simulink® Coder™.

7. Findings and Evaluation

The proposed LFC system was initially developed using MATLAB Simulink, allowing for the analysis of load frequency response in the marine grid by introducing additional load variations. To replicate sudden changes in marine load, three distinct load patterns (gradual incremental load, ramp load, and unsymmetrical load) were generated by the MATLAB Simulink's signal builder block. Figure 6 illustrates the load variation profile. To evaluate the performance of the proposed LFC, the ITAE and ITSE parameters were employed [86]. The responses of the proposed LFC remained the same for various load patterns, which established its robustness and adaptability. Figures 7–9 display the frequency responses of the proposed LFC under changing load conditions in the marine microgrid when ITAE was used as a performance indicator to minimize overshoot and oscillation. Figure 7 represents the frequency response when the PID controller's parameters were optimized using PSO [16]. Similarly, Figures 8 and 9 depict the frequency responses when the PID controller's parameters were optimized using GWO [31] and hybrid PSO-GWO algorithms, respectively. Initially, frequency fluctuations occurred for approximately 5 to 7 s, after which the frequency stabilized with load changes, demonstrating the stability and robustness of the proposed LFC. Based on the simulation results, the optimized frequency response of the PID controller outperforms the nonoptimized frequency response in terms of rise time, fall time, slew rate and overshoot [87]. Table 1 presents a comparison of the performance for the nonoptimized and optimized frequency responses when utilizing ITAE as the performance indicator. According to the simulation results, the frequency response of the GWO-PSO-tuned PID exhibits superior performance compared to the PID, PSO-tuned PID and GWO-tuned PID controllers [88].

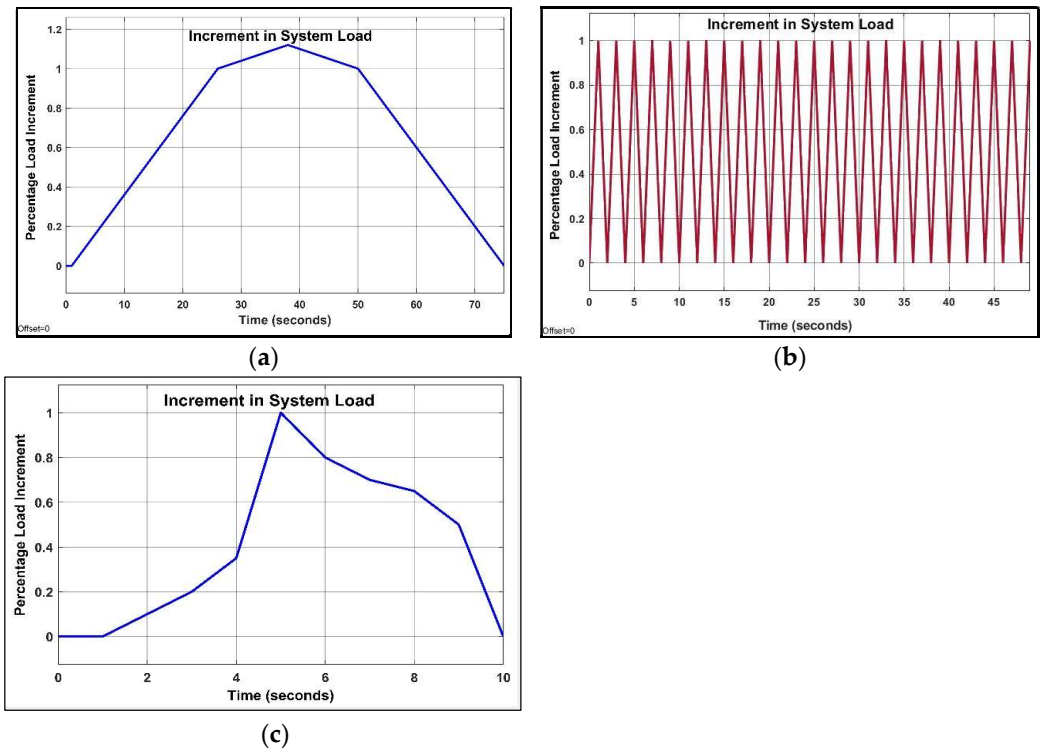


Figure 6. System load variation profile. (**a**) Gradual incremental load. (**b**) Ramp load. (**c**) Unsymmetrical load.

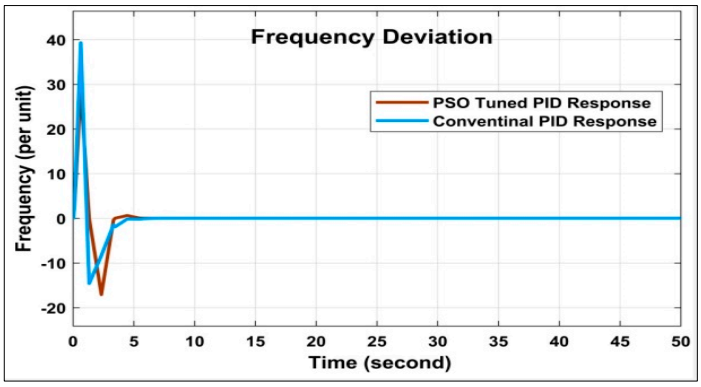


Figure 7. Frequency responses: PSO-tuned PID and conventional PID.

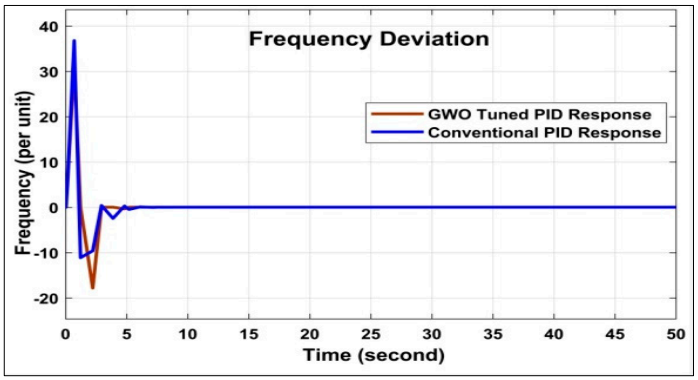


Figure 8. Frequency responses: GWO-tuned PID and conventional PID.

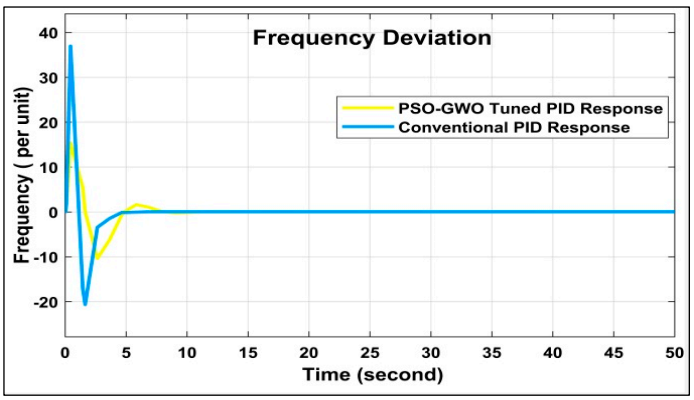


Figure 9. Frequency responses: PSO-GWO-tuned PID and conventional PID.

Table 1. ITAE-Based Proposed LFC Performance Parameters.

	For Positive Edges					For Negative Edges				
	Rise Time (ms)	**Slew Rate (/s)**	**Pre-Shoot (%)**	**Overshoot (%)**	**Undershoot (%)**	**Fall Time (ms)**	**Slew Rate (/s)**	**Pre-Shoot (%)**	**Overshoot (%)**	**Undershoot (%)**
PID	148.90	67.88	1.02	108.33	−1.54	163.95	−61.65	65.27	−0.62	0.62
PSO-tuned PID	146.59	83.39	−0.83	168.52	−5.86	134.09	−91.16	0.96	−101.85	101.85
GWO-tuned PID	518.61	48.04	0.81	0.79	−0.79	408.33	−64.01	0.79	−0.65	57.94
PSO-GWO-tuned PID	276.94	34.85	0.55	−0.45	0.45	1.80	−5.37	9.34	0.96	0.20

The frequency responses of the proposed load frequency control (LFC) system in the marine microgrid when ITSE was employed as the performance indicator to minimize response error are depicted in Figures 10–12. These figures illustrate the frequency responses obtained when optimizing the parameters of the PID controller using the PSO, GWO, and hybrid PSO-GWO algorithms, respectively. Notably, the proposed LFC demonstrated stability and robustness, as evidenced by frequency fluctuations occurring only during the initial 5 to 7 s and subsequently converging to zero despite load variations. The simulation results highlight the improved performance of the optimized LFC frequency response over the nonoptimized PID controller, specifically in terms of rise time, fall time, slew rate and overshoot [87]. Table 2 provides an overview of the performance of both nonoptimized and optimized frequency responses, utilizing ITSE as the performance criterion. The frequency response of the GWO-PSO-tuned PID exhibits superior performance compared to the PID, PSO-tuned PID and GWO-tuned PID controllers. Figure 13 displays the HIL (hardware-in-loop) real-time simulation setup, while Figure 14 showcases the control desk interface of the dSPACE 1104 which is utilized for displaying the simulation results on the workstation monitor.

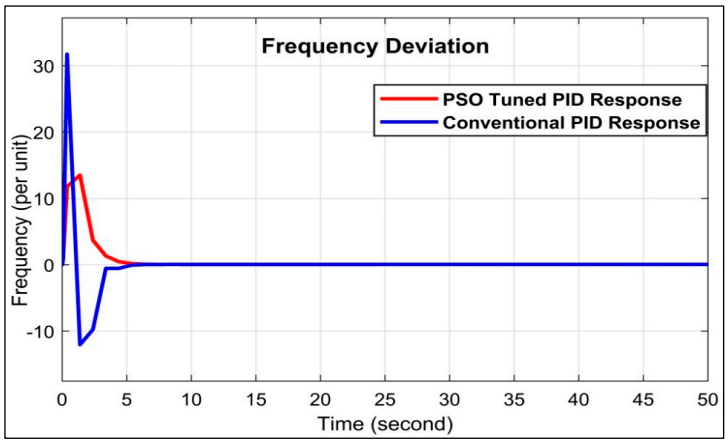


Figure 10. Frequency responses: PSO-tuned PID and conventional PID.

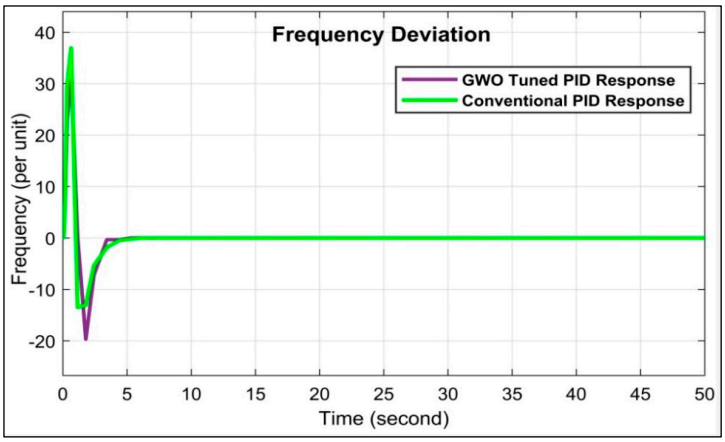


Figure 11. Frequency responses: GWO-tuned PID and conventional PID.

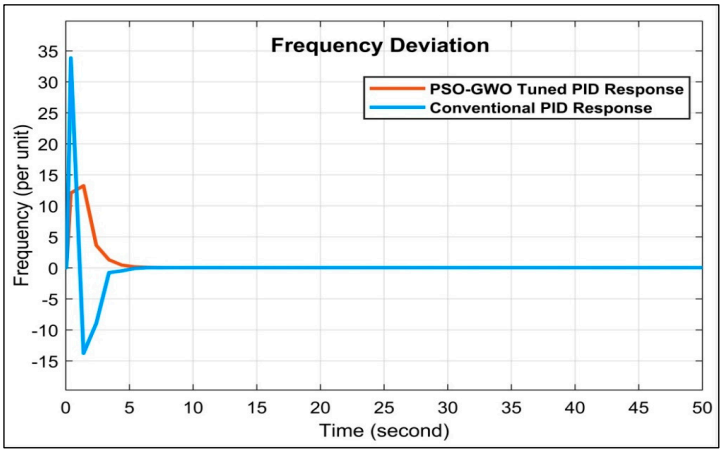


Figure 12. Frequency responses: PSO-GWO-tuned PID and conventional PID.

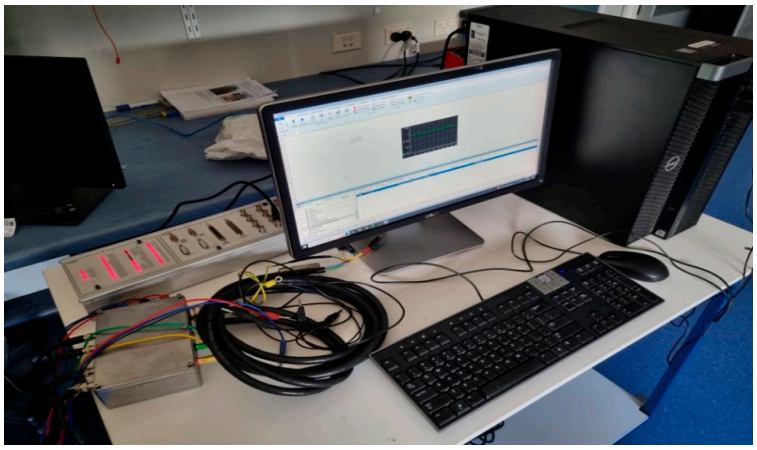


Figure 13. dSpace 1104-based HIL real-time simulation setup.

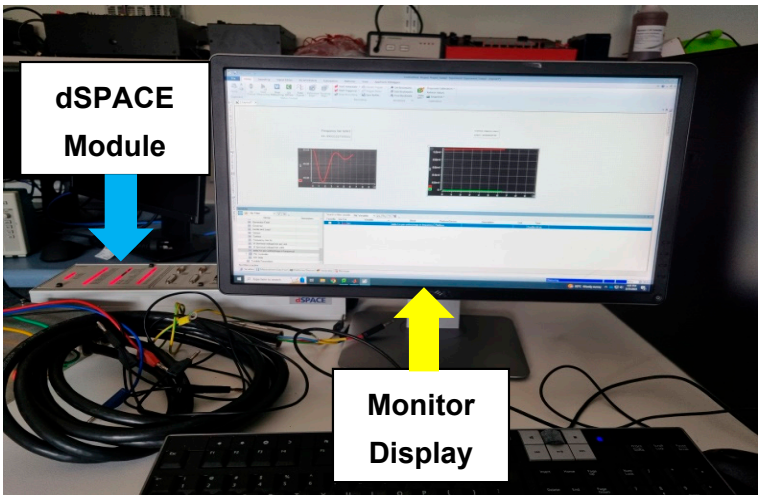


Figure 14. Real-time simulation with dSpace 1104.

Table 2. ITSE-Based Proposed LFC Performance Parameters.

	For Positive Edges					For Negative Edges				
	Rise Time (ms)	**Slew Rate (/s)**	**Pre-Shoot (%)**	**Overshoot (%)**	**Undershoot (%)**	**Fall Time (ms)**	**Slew Rate (/s)**	**Pre-Shoot (%)**	**Overshoot (%)**	**Undershoot (%)**
PID	148.90	67.88	1.02	108.33	−1.54	163.95	−61.65	65.27	−0.62	0.62
PSO-tuned PID	260.69	36.08	0.58	−0.47	0.47	1.81	−5.20	14.37	0.99	0.22
GWO-tuned PID	87.23	61.32	1.97	237.94	−237.94	86.45	−61.88	373.08	−1.97	1.97
PSO-GWO-tuned PID	260.61	36.08	0.56	−0.43	0.43	1.80	−5.25	14.37	0.82	0.39

8. Conclusions

In this study, a load frequency controller has been proposed for marine microgrids with the aim of incorporating renewable energy sources and mitigating greenhouse gas emissions. However, the presence of intermittent renewables and nonlinear loads in isolated hybrid marine microgrids can lead to frequency deviations. To address this, the proposed LFC utilizes a conventional proportional integral derivative controller and employs metaheuristic algorithms, such as PSO, GWO and hybrid PSO-GWO, for optimization. The LFC design is based on the transfer functions of various standalone hybrid marine microgrid components. A performance evaluation was carried out using integral time absolute error and integral time square error as performance indices. Hardware-in-loop real-time simulations were conducted using a DS 1104 R&D controller board for validation purposes. The simulation results showcased the superiority of the optimized frequency response achieved by the proposed LFC compared to the nonoptimized LFC controller. In particular, improvements were observed in terms of rise time, fall time, slew rate and overshoot. The hybrid PSO-GWO algorithm emerges as the most effective for optimizing the PID parameters. The simulation outcomes validate the stability and robustness of the proposed controller, affirming its potential for practical implementation in marine microgrids.

9. Discussion

The primary objective of this research was to develop a simulation-based load frequency control for an isolated marine microgrid. However, it is important to acknowledge the limitations of the proposed approach when compared to real-world systems. The real-time validation of the LFC design using the dSPACE environment provides valuable insights but may not fully capture the complexities and nuances of a real-world system. Furthermore, the simulated LFC approach is based on a set of assumptions and limitations that might not completely reflect the intricacies of a real-world system. As a result, there is a possibility of discrepancies in LFC performance due to unaccounted system dynamics, measurement errors or other factors. It is crucial to recognize that simulations typically utilize synthetic data, which may not fully capture the variability and complexity present in real-world data. Consequently, generalizing findings and validating simulation results in real-world LFC systems can be challenging.

To address these limitations, future research will focus on enhancing the proposed LFC design topology to ensure robustness, reliability and adaptability for intelligent LFC deployment in marine microgrids. This will involve considering additional system dynamics, accounting for measurement errors and incorporating real-world data variability. Moreover, further analysis will be conducted to evaluate the applicability of the proposed LFC in real-world scenarios, allowing for a comprehensive validation of the simulation-based design.

Author Contributions: Conceptualization and methodology, S.A. Preparation of the software-based simulated model and simulation results, R.B.R. Justification, visualization and formal analysis of the simulation results, S.A., R.B.R. and S.J.A. Draft preparation, review and editing, R.B.R., S.A. and S.J.A. All authors have read and agreed to the published version of the manuscript.

Funding: This research received no external funding.

Data Availability Statement: The data presented in this study are available on request from the corresponding author. The data are not publicly available due to the authors own the right of preventing the misuse or modification of the research data as an intellectual property. Since the research is still going on the proposed topic, the authors will not provide access to the full dataset until the research is finalized.

Conflicts of Interest: The authors declare no conflict of interest.

References

1. Malla, U. Design and Sizing of Battery System for Electric Yacht and Ferry. *Int. J. Interact. Des. Manuf.* **2020**, *14*, 137–142. [CrossRef]
2. Banki, T.; Faghihi, F.; Soleymani, S. Frequency Control of an Island Microgrid Using Reset Control Method in the Presence of Renewable Sources and Parametric Uncertainty. *Syst. Sci. Control Eng.* **2020**, *8*, 500–507. [CrossRef]
3. Lasseter, R.H.; Eto, J.H.; Schenkman, B.; Stevens, J.; Vollkommer, H.; Klapp, D.; Linton, E.; Hurtado, H.; Roy, J. CERTS Microgrid Laboratory Test Bed. *IEEE Trans. Power Deliv.* **2011**, *26*, 325–332. [CrossRef]
4. Roslan, M.F.; Hannan, M.A.; Ker, P.J.; Mannan, M.; Muttaqi, K.M.; Mahlia, T.I. Microgrid Control Methods toward Achieving Sustainable Energy Management: A Bibliometric Analysis for Future Directions. *J. Clean. Prod.* **2022**, *348*, 131340. [CrossRef]
5. Choudhary, A.K.; Prakash, S. Energy Management and Ancillary Services for Shipboard Microgrid. Master's Thesis, Thapar Institute of Technology, Punjab, India, 2019.
6. Jin, Z.; Sulligoi, G.; Cuzner, R.; Meng, L.; Vasquez, J.C.; Guerrero, J.M. Next-Generation Shipboard DC Power System: Introduction Smart Grid and Dc Microgrid Technologies into Maritime Electrical Netowrks. *IEEE Electrif. Mag.* **2016**, *4*, 45–57. [CrossRef]
7. Khooban, M.H.; Dragicevic, T.; Blaabjerg, F.; Delimar, M. Shipboard Microgrids: A Novel Approach to Load Frequency Control. *IEEE Trans. Sustain. Energy* **2017**, *9*, 843–852. [CrossRef]
8. Ahshan, R. Renewable Sources Based Micro-Grid Control Schemes and Reliability Modeling. Ph.D. Dissertation, Memorial University of Newfoundland, St. John's, NL, Canada, 2013. Available online: https://www.semanticscholar.org/paper/Renewable-sources-based-micro-grid-control-schemes-ahshan/9ae893989ab0dec497bb1ed5d1b157b87ad2371b (accessed on 5 April 2023).
9. Khalid, M.; Savkin, A.V. Model Predictive Control Based Efficient Operation of Battery Energy Storage System for Primary Frequency Control. In Proceedings of the 2010 11th International Conference on Control Automation Robotics & Vision, Singapore, 7–10 December 2010; pp. 2248–2252.
10. Sahu, P.R.; Lenka, R.K.; Khadanga, R.K.; Hota, P.K.; Panda, S.; Ustun, T.S. Power System Stability Improvement of FACTS Controller and PSS Design: A Time-Delay Approach. *Sustainability* **2022**, *14*, 14649. [CrossRef]
11. Zhang, R.; Hredzak, B. Distributed Control System With Aperiodic Sampled Time-Delayed Data for Batteries and Renewable Energy Sources in Microgrid. *IEEE Trans. Sustain. Energy* **2020**, *11*, 1013–1022. [CrossRef]
12. Ghosh, A.; Singh, O.; Ray, A.K.; Jamshidi, M. A Gravitational Search Algorithm-Based Controller for Multiarea Power Systems: Conventional and Renewable Sources With Variable Load Disturbances and Perturbed System Parameters. *IEEE Syst. Man Cybern. Mag.* **2021**, *7*, 20–38. [CrossRef]
13. Annamraju, A.; Nandiraju, S. A Novel Fuzzy Tuned Multistage PID Approach for Frequency Dynamics Control in an Islanded Microgrid. *Int. Trans. Electr. Energy Syst.* **2020**, *30*, e12674. [CrossRef]
14. Yammani, C.; Maheswarapu, S. Load Frequency Control of Multi-Microgrid System Considering Renewable Energy Sources Using Grey Wolf Optimization. *Smart Sci.* **2019**, *7*, 198–217. [CrossRef]
15. Nivetha, G.; Nittika, A.M.; Sarumathi, S.; Sneka, S. Energy Management Based on Virtual Generation in DC Micro Grid Using Solar Power. In Proceedings of the 2022 8th International Conference on Advanced Computing and Communication Systems (ICACCS), Coimbatore, India, 25–26 March 2022; p. 1823.
16. Shouran, M. Load Frequency Control for Multi-Area Interconnected Power System Using Artificial Intelligent Controllers. Ph.D. Thesis, Cardiff University, Cardiff, WA, USA, 2022.
17. Sebastián, R. Improved Operation and Stability of a Wind-Hydro Microgrid by Means of a Li-Ion Battery Energy Storage. *Energies* **2022**, *15*, 9230. [CrossRef]
18. Mi, Y.; Chen, B.; Cai, P.; He, X.; Liu, R.; Yang, X. Frequency Control of a Wind-Diesel System Based on Hybrid Energy Storage. *Prot. Control Mod. Power Syst.* **2022**, *7*, 31. [CrossRef]
19. Teo, T.T.; Logenthiran, T.; Woo, W.L.; Abidi, K.; John, T.; Wade, N.S.; Greenwood, D.M.; Patsios, C.; Taylor, P.C. Optimization of Fuzzy Energy-Management System for Grid-Connected Microgrid Using NSGA-II. *IEEE Trans. Cybern.* **2021**, *51*, 5375–5386. [CrossRef] [PubMed]
20. Yang, J.; Sun, X.; Liao, K.; He, Z.; Cai, L. Model Predictive Control Based Load Frequency Control for Power Systems with Wind Turbine Generators. *IET Renew. Power Gener.* **2019**, *13*, 2871–2879. [CrossRef]
21. Pandey, S.K.; Mohanty, S.R.; Kishor, N. A Literature Survey on Load–Frequency Control for Conventional and Distribution Generation Power Systems. *Renew. Sustain. Energy Rev.* **2013**, *25*, 318–334. [CrossRef]

22. Coban, H.H.; Rehman, A.; Mousa, M. Load Frequency Control of Microgrid System by Battery and Pumped-Hydro Energy Storage. *Water* **2022**, *14*, 1818. [CrossRef]
23. Wang, S.-Y.; Hong, C.-M.; Yang, W.-T.; Liu, C.-C. Constructing a Sliding Regime for Load-Frequency Control of an Interconnected Hydrothermal Power System. *Int. J. Syst. Sci.* **1995**, *26*, 467–480. [CrossRef]
24. Dahiya, P.; Mukhija, P.; Saxena, A.; Arya, Y. Comparative Performance Investigation of Optimal Controller for AGC of Electric Power Generating Systems. *Automatika* **2016**, *57*, 902–921. [CrossRef]
25. Mondal, A.; Latif, A.; Das, D.C.; Hussain, S.M.S.; Al-Durra, A. Frequency Regulation of Hybrid Shipboard Microgrid System Using Butterfly Optimization Algorithm Synthesis Fractional-Order Controller. *Int. J. Numer. Model. Electron. Netw. Devices Fields* **2022**, e3058. [CrossRef]
26. Tungadio, D.H.; Sun, Y. Load Frequency Controllers Considering Renewable Energy Integration in Power System. *Energy Rep.* **2019**, *5*, 436–453. [CrossRef]
27. Kwon, K.; Park, D.; Zadeh, M.K. Load Frequency-Based Power Management for Shipboard DC Hybrid Power Systems. In Proceedings of the 2020 IEEE 29th International Symposium on Industrial Electronics (ISIE), Delft, The Netherlands, 17–19 June 2020; pp. 142–147.
28. Latif, A.; Hussain, S.M.S.; Das, D.C.; Ustun, T.S. State-of-the-Art of Controllers and Soft Computing Techniques for Regulated Load Frequency Management of Single/Multi-Area Traditional and Renewable Energy Based Power Systems. *Appl. Energy* **2020**, *266*, 114858. [CrossRef]
29. Latif, A.; Hussain, S.; Das, D.; Ustun, T.S.; Iqbal, A. A Review on Fractional Order (FO) Controllers' Optimization for Load Frequency Stabilization in Power Networks. *Energy Rep.* **2021**, *7*, 4009–4021. [CrossRef]
30. Latif, A.; Hussain, S.; Das, D.; Ustun, T.S. Double Stage Controller Optimization for Load Frequency Stabilization in Hybrid Wind-Ocean Wave Energy Based Maritime Microgrid System. *Appl. Energy* **2021**, *282*, 116171. [CrossRef]
31. Guha, D.; Roy, P.; Banerjee, S. Grasshopper Optimization Algorithm-Scaled Fractional-Order PI-D Controller Applied to Reduced-Order Model of Load Frequency Control System. *Int. J. Model. Simul.* **2019**, *40*, 217–242. [CrossRef]
32. Malik, S.; Suhag, S. A Coordinated Control Strategy for Frequency Regulation in Hybrid Shipboard Power System Using Novel Salp Swarm Algorithm Tuned Fractional Controller. *Int. J. Ambient Energy* **2021**, *43*, 5638–5653. [CrossRef]
33. Vafamand, N.; Khooban, M.H.; Dragičević, T.; Boudjadar, J.; Asemani, M.H. Time-Delayed Stabilizing Secondary Load Frequency Control of Shipboard Microgrids. *IEEE Syst. J.* **2019**, *13*, 3233–3241. [CrossRef]
34. Dahiya, P.; Sharma, V.; Naresh, R. Hybridized Gravitational Search Algorithm Tuned Sliding Mode Controller Design for Load Frequency Control System with Doubly Fed Induction Generator Wind Turbine. *Optim. Control Appl. Methods* **2017**, *38*, 993–1003. [CrossRef]
35. Arya, Y. A New Optimized Fuzzy FOPI-FOPD Controller for Automatic Generation Control of Electric Power Systems. *J. Frankl. Inst.* **2019**, *356*, 5611–5629. [CrossRef]
36. Guha, D.; Roy, P.K.; Banerjee, S. Adaptive Fractional-Order Sliding-Mode Disturbance Observer-Based Robust Theoretical Frequency Controller Applied to Hybrid Wind–Diesel Power System. *ISA Trans.* **2023**, *133*, 160–183. [CrossRef]
37. Jin, L.; Zhang, C.-K.; He, Y.; Jiang, L.; Wu, M. Delay-Dependent Stability Analysis of Multi-Area Load Frequency Control with Enhanced Accuracy and Computation Efficiency. *IEEE Trans. Power Syst.* **2019**, *34*, 3687–3696. [CrossRef]
38. Franklin, R.V.; Abdul Kareem, P.F. Frequency Regulation in Conventional, Deregulated and Microgrid Systems: A Review on Designs, Strategies, Techniques and Related Aspects. *IETE J. Res.* **2022**, 1–19. [CrossRef]
39. Anwar, M.N.; Pan, S. A New PID Load Frequency Controller Design Method in Frequency Domain through Direct Synthesis Approach. *Int. J. Electr. Power Energy Syst.* **2015**, *67*, 560. [CrossRef]
40. Cassol, G.O.; Dubljevic, S. Discrete Output Regulator Design for the Linearized Saint–Venant–Exner Model. *Processes* **2020**, *8*, 915. [CrossRef]
41. Mahmood, H.; Michaelson, D.; Jiang, J. Strategies for Independent Deployment and Autonomous Control of PV and Battery Units in Islanded Microgrids. *IEEE J. Emerg. Sel. Top. Power Electron.* **2015**, *3*, 742–755. [CrossRef]
42. Dash, P.; Saikia, L.C.; Sinha, N. Automatic Generation Control of Multi Area Thermal System Using Bat Algorithm Optimized PD–PID Cascade Controller. *Int. J. Electr. Power Energy Syst.* **2015**, *68*, 364–372. [CrossRef]
43. Bhullar, A.K.; Kaur, R.; Sondhi, S. Enhanced Crow Search Algorithm for AVR Optimization. *Soft Comput* **2020**, *24*, 11957–11987. [CrossRef]
44. Castaignet, D.B. Model Predictive Control of Trailing Edge Flaps on a Wind Turbine Blade. In Proceedings of the 2011 American Control Conference, San Francisco, CA, USA, 29 June–1 July 2011.
45. Ersdal, A.M.; Imsland, L.; Uhlen, K. Model Predictive Load-Frequency Control. *IEEE Trans. Power Syst.* **2016**, *31*, 777–785. [CrossRef]
46. Ma, M.; Zhang, C.; Liu, X.; Chen, H. Distributed Model Predictive Load Frequency Control of the Multi-Area Power System After Deregulation. *IEEE Trans. Ind. Electronics* **2016**, *64*, 5129–5139. [CrossRef]
47. Muyizere, D.; Letting, L.K.; Munyazikwiye, B.B. Effects of Communication Signal Delay on the Power Grid: A Review. *Electronics* **2022**, *11*, 874. [CrossRef]
48. Khooban, M.H.; Niknam, T. A New Intelligent Online Fuzzy Tuning Approach for Multi-Area Load Frequency Control: Self Adaptive Modified Bat Algorithm. *Int. J. Electr. Power Energy Syst.* **2015**, *71*, 254–261. [CrossRef]

49. Shayeghi, H.; Shayanfar, H.A.; Jalili, A. Load Frequency Control Strategies: A State-of-the-Art Survey for the Researcher. *Energy Convers. Manag.* **2009**, *50*, 344–353. [CrossRef]
50. Dash, P.; Saikia, L.C.; Sinha, N. Comparison of Performances of Several FACTS Devices Using Cuckoo Search Algorithm Optimized 2DOF Controllers in Multi-Area AGC. *Int. J. Electr. Power Energy Syst.* **2015**, *65*, 316–324. [CrossRef]
51. Guha, D.; Roy, P.K.; Banerjee, S. Optimal Tuning of 3 Degree-of-Freedom Proportional-Integral-Derivative Controller for Hybrid Distributed Power System Using Dragonfly Algorithm. *Comput. Electr. Eng.* **2018**, *72*, 137–153. [CrossRef]
52. Al-Hamouz, Z.M.; Al-Duwaish, H.N. A New Load Frequency Variable Structure Controller Using Genetic Algorithms. *Electr. Power Syst. Res.* **2000**, *55*, 1–6. [CrossRef]
53. Chen, D.; Zhang, G.; Yao, C. PSO Algorithm Based PID Parameters Optimization of Hydraulic Screwdown System of Cold Strip Mill. In Proceedings of the 2011 International Conference on Fluid Power and Mechatronics, Beijing, China, 17–20 August 2011; pp. 113–116.
54. Raju, M.; Gupta, M.K.; Bhanot, N.; Sharma, V.S. A Hybrid PSO–BFO Evolutionary Algorithm for Optimization of Fused Deposition Modelling Process Parameters. *J. Intell. Manuf.* **2019**, *30*, 2743–2758. [CrossRef]
55. Ostadian, R.; Ramoul, J.; Biswas, A.; Emadi, A. Intelligent Energy Management Systems for Electrified Vehicles: Current Status, Challenges, and Emerging Trends. *IEEE Open J. Veh. Technol.* **2020**, *1*, 279–295. [CrossRef]
56. Chen, W.; Bazzi, A.; Hare, J.; Gupta, S. Real-Time Integrated Model of a Micro-Grid with Distributed Clean Energy Generators and Their Power Electronics. In Proceedings of the 2016 IEEE Applied Power Electronics Conference and Exposition (APEC), Long Beach, CA, USA, 20–24 March 2016; pp. 2666–2672.
57. Cuculić, A.; Vučetić, D.; Prenc, R.; Ćelić, J. Analysis of Energy Storage Implementation on Dynamically Positioned Vessels. *Energies* **2019**, *12*, 444. [CrossRef]
58. Kamen, E.W.; Heck, B.S. *Fundamentals of Signals and Systems Using the Web and MATLAB: Pearson New International Edition*, 3rd ed.; Prentice-Hall, Inc.: Hoboken, NJ, USA, 2006. Available online: https://dokumen.pub/fundamentals-of-signals-and-systems-using-the-web-and-matlab-pearson-new-international-edition-3rd-ed-1292025980-9781292025988.html (accessed on 6 April 2023).
59. Andújar, J.M.; Segura, F.; Vasallo, M.J. A Suitable Model Plant for Control of the Set Fuel Cell−DC/DC Converter. *Renew. Energy* **2008**, *33*, 813–826. [CrossRef]
60. Maswood, A.I.; Nandakumar, S. Developing a PEM Fuel Cell Electrical Equivalent Circuit. In Proceedings of the 2008 IEEE International Conference on Sustainable Energy Technologies, Singapore, 24–27 November 2008; pp. 1166–1171.
61. Xue, X.D.; Cheng, K.W.E.; Sutanto, D. Unified Mathematical Modelling of Steady-State and Dynamic Voltage–Current Characteristics for PEM Fuel Cells. *Electrochim. Acta* **2006**, *52*, 1135–1144. [CrossRef]
62. Akinci, T.C.; Seker, S.; Dursun, E.; Kilic, O. Noise Identification Based on Spectral Analysis and Noisy Transfer Function Approach for Fuel Cells. *Noise Mapp.* **2020**, *7*, 14–21. [CrossRef]
63. An Elite LOA-TFWO Approach for Load-Frequency Control of Islanded Micro-Grids Incorporating Renewable Sources. Available online: https://ijettjournal.org/archive/ijett-v70i10p217 (accessed on 6 April 2023).
64. Annamraju, A.; Bhukya, L.; Nandiraju, S. Robust Frequency Control in a Standalone Microgrid: An Adaptive Fuzzy Based Fractional Order Cascade PD-PI Approach. *Adv. Control Appl.* **2021**, *3*, e72. [CrossRef]
65. Li, H.; Wang, X.; Xiao, J. Adaptive Event-Triggered Load Frequency Control for Interconnected Microgrids by Observer-Based Sliding Mode Control. *IEEE Access* **2019**, *7*, 68271–68280. [CrossRef]
66. Singla, H.; Kumar, A. LQR Based Load Frequency Control with SMES in Deregulated Environment. In Proceedings of the 2012 Annual IEEE India Conference (INDICON), Kochi, India, 7–9 December 2012; pp. 286–292.
67. Al-Mashakbeh, A.S.O. Modern Control Design of Power System. *Aust. J. Basic Appl. Sci.* **2009**, *3*, 4267–4273.
68. Mobarak, Y.A.; Deraz, S.A.; Dessouki, M.E.; Almazmomi, R. Optimal Control Techniques in Applicable Values of Turbine Speed Governor Regulation. *SSRG Int. J. Electr. Electron. Eng.* **2015**, *2*, 24–35.
69. Khachay, M.; Kochetov, Y.; Pardalos, P. Mathematical Optimization Theory and Operations Research. In Proceedings of the 18th International Conference, MOTOR 2019, Ekaterinburg, Russia, 8–12 July 2019; Volume 11548, ISBN 978-3-030-22628-2.
70. Textbook: Convex Optimization Algorithms. Available online: http://www.athenasc.com/convexalg.html (accessed on 11 June 2023).
71. Körkel, S.; Qu, H.; Rücker, G.; Sager, S. Derivative Based vs. Derivative Free Optimization Methods for Nonlinear Optimum Experimental Design. In *Current Trends in High Performance Computing and Its Applications, Proceedings of the International Conference on High Performance Computing and Applications, Shanghai, China, 8–10 August 2004*; Springer: Berlin/Heidelberg, Germany, 2005; pp. 339–344, ISBN 978-3-540-25785-1.
72. Shin, Y.; Darbon, J.; Karniadakis, G.E. A Caputo Fractional Derivative-Based Algorithm for Optimization. *arXiv* **2021**, arXiv:2104.02259.
73. Kaur, S.; Kumar, Y.; Koul, A.; Kumar Kamboj, S. A Systematic Review on Metaheuristic Optimization Techniques for Feature Selections in Disease Diagnosis: Open Issues and Challenges. *Arch. Comput. Methods Eng.* **2023**, *30*, 1863–1895. [CrossRef]
74. Wong, W.; Ming, C.I. A Review on Metaheuristic Algorithms: Recent Trends, Benchmarking and Applications. In Proceedings of the 2019 7th International Conference on Smart Computing & Communications (ICSCC), Miri, Sarawak, Malaysia, 28–30 June 2019; pp. 1–5.

75. Kumar, A. Chapter 5—Application of Nature-Inspired Computing Paradigms in Optimal Design of Structural Engineering Problems—A Review. In *Nature-Inspired Computing Paradigms in Systems*; Mellal, M.A., Pecht, M.G., Eds.; Intelligent Data-Centric Systems; Academic Press: Cambridge, MA, USA, 2021; pp. 63–74, ISBN 978-0-12-823749-6.
76. Gupta, S.; Abderazek, H.; Yıldız, B.S.; Yildiz, A.R.; Mirjalili, S.; Sait, S.M. Comparison of Metaheuristic Optimization Algorithms for Solving Constrained Mechanical Design Optimization Problems. *Expert Syst. Appl.* **2021**, *183*, 115351. [CrossRef]
77. Dada, E.; Joseph, S.; Oyewola, D.; Fadele, A.; Chiroma, H.; Abdulhamid, S. Application of Grey Wolf Optimization Algorithm: Recent Trends, Issues, and Possible Horizons. *Gazi Univ. J. Sci.* **2022**, *35*, 485–504. [CrossRef]
78. Hou, Y.; Gao, H.; Wang, Z.; Du, C. Improved Grey Wolf Optimization Algorithm and Application. *Sensors* **2022**, *22*, 3810. [CrossRef]
79. Lee, K.Y.; Park, J. Application of Particle Swarm Optimization to Economic Dispatch Problem: Advantages and Disadvantages. In Proceedings of the 2006 IEEE PES Power Systems Conference and Exposition, Atlanta, GA, USA, 29 October–1 November 2006; pp. 188–192.
80. Gaing, Z.-L. Particle Swarm Optimization to Solving the Economic Dispatch Considering the Generator Constraints. *IEEE Tans. Power Syst. IEEE Trans.* **2003**, *18*, 1187–1195. [CrossRef]
81. Kora, P.; Kalva, S.R. Hybrid Bacterial Foraging and Particle Swarm Optimization for Detecting Bundle Branch Block. *SpringerPlus* **2015**, *4*, 481. [CrossRef] [PubMed]
82. Design of Integral SMC and Fuzzy Pid Controller for Voltage Control of a DC-DC Buck-Boost Converter. National Academic Digital Repository of Ethiopia. Available online: https://nadre.ethernet.edu.et/record/4169#.ZC2gZfZBw2w (accessed on 6 April 2023).
83. Raj, T.D.; Kumar, C.; Kotsampopoulos, P.; Fayek, H.H. Load Frequency Control in Two-Area Multi-Source Power System Using Bald Eagle-Sparrow Search Optimization Tuned PID Controller. *Energies* **2023**, *16*, 2014. [CrossRef]
84. Obando, C.; Rojas, R.; Ulloa, F.; Camacho, O. Dual-Mode Based Sliding Mode Control Approach for Nonlinear Chemical Processes. *ACS Omega* **2023**, *8*, 9511–9525. [CrossRef] [PubMed]
85. Lal, D.; Barisal, A.; Tripathy, M. Load Frequency Control of Multi Area Interconnected Microgrid Power System Using Grasshopper Optimization Algorithm Optimized Fuzzy PID Controller. In Proceedings of the 2018 Recent Advances on Engineering, Technology and Computational Sciences (RAETCS), Allahabad, India, 6 February 2018; p. 6.
86. Ahmed, N.A.; Abdul Rahman, S.; Alajmi, B.N. Optimal Controller Tuning for P&O Maximum Power Point Tracking of PV Systems Using Genetic and Cuckoo Search Algorithms. *Int. Trans. Electr. Energy Syst.* **2021**, *31*, e12624. [CrossRef]
87. Pattnaik, S.; Kumar, M.R.; Mishra, S.K.; Gautam, S.P.; Appasani, B.; Ustun, T.S. DC Bus Voltage Stabilization and SOC Management Using Optimal Tuning of Controllers for Supercapacitor Based PV Hybrid Energy Storage System. *Batteries* **2022**, *8*, 186. [CrossRef]
88. Shrivastava, S.; Singh, V.; Dohare, R.; Singh, S.; Chauhan, D. PID Tuning for Position Control of DC Servo-Motor Using TLBO. *Int. J. Adv. Technol. Eng. Explor.* **2016**, *4*, 23–27. [CrossRef]

Disclaimer/Publisher's Note: The statements, opinions and data contained in all publications are solely those of the individual author(s) and contributor(s) and not of MDPI and/or the editor(s). MDPI and/or the editor(s) disclaim responsibility for any injury to people or property resulting from any ideas, methods, instructions or products referred to in the content.